International Journal of Energy Horizon 01 (2025) 1-7

International Journal of Energy Horizon

journal homepage: https://dergipark.org.tr/tr/pub/ijeh

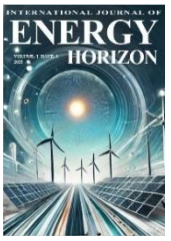

Research Paper

A Parametric and Performance-Based CFD Investigation of The Effect of Cavity Geometry and Location of Injector on Flame Stabilization in Supersonic Flow

Barış AKIN[1], Mohammed ALOBEID[2,*], Ahmed Emin KILIÇ[3]

[1,2,3]Ankara Yıldırım Beyazıt University, Faculty of Engineering and Natural Science, Mechanical Engineering Department, Ankara, 06010, Turkey
[1]ORCID No:0009-0002-0680-9890
[2]ORCID No:0009-0001-9442-4650
[3]ORCID No:0000-0002-8472-9426

ARTICLE INFO

Article History:

Received:11 June 2025
Revised:18 June 2025
Accepted:19 June 2025
Available online:30 June 2025

Keywords:

Scramjet combustion
Cavity geometry
Fuel injection location
Flame stabilization
CFD simulation

ABSTRACT

Scramjet (Supersonic Combustion Ramjet) engines are a key propulsion technology for hypersonic flight, where stable combustion and efficient fuel–air mixing under supersonic conditions remain fundamental challenges. This study presents a two-dimensional computational fluid dynamics (CFD) investigation to optimize cavity geometry and fuel injection configurations in a scramjet combustor to enhance mixing and flame stabilization. Rectangular and trapezoidal cavity geometries were assessed under varying hydrogen injection pressures (1, 2, and 3 atm) and locations (top, middle, and bottom) using ANSYS Fluent. A density-based solver incorporating the SST k-ω turbulence model and the Eddy Dissipation Model was employed to simulate reactive flow dynamics. Validation of the numerical model was performed through comparison with experimental data, ensuring mesh independence and agreement on normalized pressure profiles. Results showed that injection location and cavity geometry significantly influence flow recirculation, fuel retention, and temperature distribution. The middle injection at 2 atm in the rectangular cavity yielded the most uniform vortex formation and the highest combustion efficiency. In contrast, top injection configurations consistently resulted in poor flame holding due to bypassing of the cavity. For the trapezoidal cavity, middle and bottom injections at 2 atm exhibited comparable mixing behavior, albeit with lower peak temperatures. Overall, the rectangular cavity with centerline injection at 2 atm demonstrated optimal performance for sustained combustion in supersonic flow. These findings contribute to the design of efficient flameholders in scramjet systems, offering insights for improved performance in future hypersonic propulsion applications.

1. INTRODUCTION

Supersonic Combustion Ramjet (SCRAMJET) engines are among the most promising candidates for hypersonic propulsion, capable of operating efficiently at speeds above Mach 5. Unlike traditional rocket systems that rely on onboard oxidizers—leading to high propellant mass fractions and limited reusability—SCRAMJETs utilize atmospheric oxygen for combustion. This significantly improves payload capacity and reduces launch costs [1].

While ramjets and turbojets perform well at lower supersonic speeds, their effectiveness diminishes at hypersonic regimes due to increased flow separation, shock–boundary layer interaction, and combustion inefficiencies. SCRAMJETs overcome this by sustaining supersonic combustion, enabling continuous thrust at high Mach numbers. Nonetheless, key engineering hurdles—such as flame stabilization, efficient fuel–air mixing in ultra-short residence times, high thermal loads on structural materials, and thermal management—must be resolved [2–4].

Flame stabilization in scramjets is particularly challenging due to the supersonic flow and short interaction times. Among the studied strategies, cavity-based flameholders offer a passive means of anchoring flames via recirculation zones that slow and trap the flame within the combustor [5]. Experimental and numerical investigations have shown that rectangular, trapezoidal, and strut-assisted cavities can enhance flame stabilization under high-speed flows [5-7]. For instance, Liu et al. demonstrated ignition and flame stabilization in an ethylene-fueled cavity scramjet using high-speed imaging and pressure diagnostics [8]. Moreover, recent DNS and LES studies have characterized turbulence–flame interactions within cavity shear layers, clarifying how inflow turbulence impacts flame topology and stability[3-4] .

*Corresponding author
E-mail address: mohammed.alobed@gmail.com
journal homepage: https://dergipark.org.tr/tr/pub/ijeh

Efficient fuel mixing remains crucial under extreme supersonic conditions. Studies by Relangi et al. explored how axisymmetric cavities with angled and transverse injections affect mixing, revealing improvements in uniformity and performance [9]. Li et al. experimentally demonstrated that adding cavity-floor injection in ethylene–air flows can extend stable ignition limits by boosting residence time [10]. Other researchers have examined strut-based injectors and their interaction with shock-generated vortices, emphasizing the trade-offs between enhanced mixing and total pressure losses [11].

Combustion dynamics, including thermoacoustic instability and oscillation, directly impact durability and control. Jeong et al. applied POD techniques to high-speed CH* chemiluminescence data, identifying dominant oscillation modes in cavity combustors at Mach 2.5 [12]. Newer computational models using shock-induced stabilization via parallel cavities have been shown to attenuate instabilities and maintain stable flames at high Mach regimes [13]. Meanwhile, Huang et al. reviewed turbulence modeling and CFD simulation strategies, concluding that LES combined with detailed chemistry models offers the most accurate predictions of transient processes, including thermal and combustion responses [2].

Parametric CFD studies remain essential to optimize cavity geometry, fuel injection schemes, and operational conditions. Sun et al. assessed ignition enhancement techniques for Mach 2 combustors with cavity and floor injection under varying equivalence ratios [13]. Zhang and co-workers, analyzing strut/wall injection hybrid schemes, reported fuel penetration, flame anchoring, and temperature distribution improvements, though pressure losses required further mitigation [14]. New numerical work published in late 2024 highlighted that cavity length-to-depth ratios of around 4 maximize combustion efficiency while minimizing total pressure losses [15]. Collectively, these studies inform the design of stable, high-performance supersonic combustors.

2. NUMERICAL METHODOLOGY AND COMPUTATIONAL SETUP

2.1. Geometric Model

At The combustor geometry was designed to investigate the effects of cavity shape and injection configuration on flame stabilization. Two distinct cavity geometries rectangular and trapezoidal were considered. The performance of each was evaluated based on fuel–air mixing, recirculation behavior, and combustion efficiency.

A parametric sweep was performed for three offset ratios (Du/D = 1, 2, 3), defined as the ratio of the cavity's front wall length to the rear wall length. For each offset ratio, three rear wall ramp angles (θ = 90°, 60°, and 30°) were analyzed. This allowed a systematic investigation of cavity shape on internal vortex structure and flame anchoring potential.

In all cases, hydrogen was injected through three discrete positions along the front wall—top, middle, and bottom parallel to the main airflow. Injection pressures of 1 atm, 2 atm, and 3 atm were applied to assess their effect on combustion characteristics.

The main supersonic airflow enters the domain at Mach 3, with a stagnation temperature of 1400 K and static pressure of 1 atm. The hydrogen fuel enters at Mach 1 and 300 K, under the specified pressure levels. The simulation domain was constructed to mirror typical combustor test-section dimensions found in experimental studies.

The main flow was characterized by Mach 3 and 1 atm pressure, with an inlet temperature of 1400 K. The fuel inlet was exposed to a series of extreme conditions, including temperatures of 300K and velocities of Mach 1, as well as variable pressures.

2.2. Governing Equations And Numerical Modeling Approach

The reactive supersonic flow within the scramjet combustor was modeled as a two-dimensional, steady, compressible system governed by the conservation laws of mass, momentum, and total energy. These equations were solved using ANSYS Fluent 2024 R2 with a density-based solver and an implicit formulation.

The governing equations are as follows:

1) Continuity Equation (Mass Conservation):

$$\frac{\partial \rho}{\partial t} + \nabla \cdot (\rho \vec{v}) = 0 \tag{1}$$

2) Momentum Conservation Equation:

$$\frac{\partial (\rho \vec{v})}{\partial t} + \nabla \cdot (\rho \vec{v} \vec{v}) = -\nabla p + \nabla \cdot \tau + \rho \vec{g} \tag{2}$$

where τ is the viscous stress tensor.

$$\tau_{ij} = \mu \left(\frac{\partial v_i}{\partial x_j} + \frac{\partial v_j}{\partial x_i} \right) - \frac{2}{3} \mu (\nabla \cdot \vec{v}) \delta_{ij} \tag{3}$$

3) Energy Conservation Equation:

$$\frac{\partial (\rho E)}{\partial t} + \nabla \cdot [\vec{v}(\rho E + p)] = \nabla \cdot (k_{\text{eff}} \nabla T) + \Phi + S_h \tag{4}$$

S_h: heat production term

k_{eff}: effective thermal conductivity

Φ: viscous dispersion term

E: total energy (internal energy + kinetic energy)

2.2.1. Numerical Model

In this simulation, the k-ω SST turbulence model is employed to predict the effects of disturbances within the flow field with a high degree of accuracy. This model is known for its ability to handle complex flow situations, especially in areas with strong pressure differences and during transient flow. A primary advantage of the present approach is that it offers high accuracy near the wall while maintaining a relatively low computational cost compared to other turbulence modelling methods.

The k-ω formulation is applied to enhance accuracy in near-wall regions. The k-ε is used in the outer flow regions to blend and allow the SST model to leverage the strengths of both formulations. This hybrid approach ensures robust and physically consistent turbulence modelling. The k-ω SST model is particularly suitable for high-speed flows, such as those found in scramjet combustors [16].

$$\frac{\partial}{\partial x_i}(\rho k u_i) = \frac{\partial}{\partial x_i}\left(\Gamma_k \frac{\partial k}{\partial x_j} \right) + \widetilde{G_k} - Y_k + S_k \tag{5}$$

This equation represents turbulent kinetic energy. The right side of the equation shows diffusion, production, dispersion and an additional source.

$$\frac{\partial}{\partial x_i}(\rho \omega u_i) = \frac{\partial}{\partial x_j}\left(\Gamma_\omega \frac{\partial \omega}{\partial x_j} \right) + G_\omega - Y_\omega + D_\omega + S_\omega \tag{6}$$

This equation expresses the transport of specific turbulent dispersion velocity. The symbol D_ω denotes the cross-diffusion term.

$$D_\omega = 2(1 - F_1)\rho \sigma_{\omega 2} \cdot \frac{1}{\omega} \cdot \frac{\partial k}{\partial x_j} \cdot \frac{\partial \omega}{\partial x_j} \tag{7}$$

The cross-diffusion term is an important component of the SST model and contributes to the ω equation in the transition region.

$$\Gamma_k = \mu + \frac{\mu_t}{\sigma_k}, \quad \Gamma_\omega = \mu + \frac{\mu_t}{\sigma_\omega} \tag{8}$$

The term ' Γ ' combining the contributions of viscosity and turbulent viscosity in turbulent flows.

$$\mu_t = \frac{\rho k}{\omega} \tag{9}$$

The turbulent viscosity definition is used in the SST model. Some versions include an SST mixing function.

$$\frac{\partial}{\partial t}(\rho Y_i) + \nabla \cdot (\rho \vec{v} Y_i) = -\nabla \cdot \vec{J_i} + R_i + S_i \tag{10}$$

The transport equation for species 'i' includes diffusion flux, reaction production and external sources.

The combustion process in supersonic flows is significantly affected by turbulence. Considering the considerations, the eddy-dissipation reaction model was employed, incorporating the turbulence intensity in the calculations. The process under consideration is a one-stage chemical reaction between air and hydrogen, represented by the following formula: $2H_2+O_2 \rightarrow 2H_2O$.

$$R_i = \min\left(\frac{A\rho\epsilon}{k} \cdot \frac{Y_{\text{fuel}}}{\nu_{\text{fuel}}}, \frac{B\rho\epsilon}{k} \cdot \frac{Y_{\text{oxid}}}{\nu_{\text{oxid}}} \right) \tag{11}$$

The reaction rate in this equation is determined by the turbulent mixing ratio.

ν: Stoichiometric coefficient

Y_{fuel}: Mass fraction of H_2

Y_{oxid}: Mass fraction of O_2

The numerical analysis was conducted using commercial software, namely ANSYS-Fluent 2024 R2. In numerical analysis, the Coupled method was employed for the pressure-velocity pair, while the second-order UPWIND method was utilized for the discretization of the conservation equations. The convergence criteria were accepted as 10^{-5} for the mass and momentum conservation equations and 10^{-5} for the energy conservation equations. The numerical analyses were terminated when the convergence criteria were met.

2.3. Mesh & Boundary Conditions

To ensure numerical accuracy and solution stability, a high-quality structured mesh was generated, with localized refinement in the cavity region where complex recirculation and mixing phenomena are expected. The mesh quality was quantitatively evaluated based on element quality, aspect ratio, skewness, and orthogonal quality, as summarized in Table 1. The average element quality exceeded 0.95, indicating minimal distortion and excellent grid resolution in regions of interest. Skewness values remained below 0.17, and the orthogonal quality was consistently above 0.96, supporting accurate resolution of steep gradients in pressure and temperature. The computational domain, including the location of the cavity, injectors, and boundary conditions, is illustrated in Figure 1, which highlights the key regions of flow development and fuel–air interaction. Boundary conditions were applied to reflect realistic scramjet operating conditions: the main airflow was introduced at Mach 3 with a static pressure of 1 atm and a total temperature of 1400 K, while the hydrogen fuel was injected at Mach 1 and 300 K from three separate locations along the front cavity wall at pressures of 1 atm, 2 atm, and 3 atm. All walls were modeled as adiabatic and no-slip, and a pressure outlet was imposed downstream to allow unrestrained flow development. The inlet gas compositions used in all simulations are detailed in Table 2, with consistent species mass fractions applied for both air and hydrogen in each case. This meshing and boundary setup provided a robust framework for capturing the high-speed reactive flow characteristics critical to flame stabilization in scramjet cavities.

Table 1. Mesh metrics

	Min	Max	Average
Element Quality	0.91389	0.99997	0.95149
Aspect Ratio	1.0011	1.4983	1.3608
Skewness	1.6287e-006	0.16422	2.6285e-002
Orthogonal Quality	0.96694	1	0.99717

Table 2. Fluid inlet properties

Fluid	P (atm)	T (K)	Mach
Air	1	1200	3
H2	1,2,3	300	1

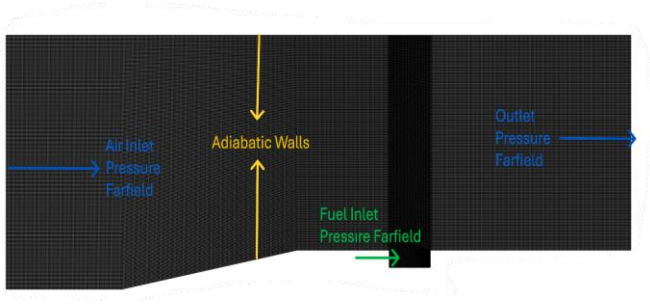

Fig.1 Computational domain

3. VALIDATION

The numerical model was validated through a two-stage process to ensure the reliability of the simulation results. First, a mesh independence study was conducted to determine the optimal number of grid elements required to achieve stable and accurate results. As shown in Figure 3(b) the normalized pressure value at the flameholder surface plateaued beyond 76,000 elements, with variations remaining below 0.1%, confirming numerical independence and justifying the selected mesh density for subsequent simulations. The second stage of validation involved direct comparison of numerical predictions with experimental data reported by Gruber et al. (2001). The experimental setup used in their study is schematically illustrated in Figure 2, including the combustor geometry and flameholder placement. Key validation metrics were extracted from the normalized pressure distribution along the flameholder surface, calculated as the ratio of local pressure to inlet pressure. A comparison of numerical and experimental results is presented in Figure 3 (a), demonstrating strong agreement in both trend and magnitude, particularly in the effective distance from the leading edge of the flameholder to the location of peak pressure. These results confirm the model's capability to accurately replicate critical flow features relevant to combustion stabilization in supersonic flow regimes. The validated mesh and numerical approach were then employed for further parametric investigations [17].

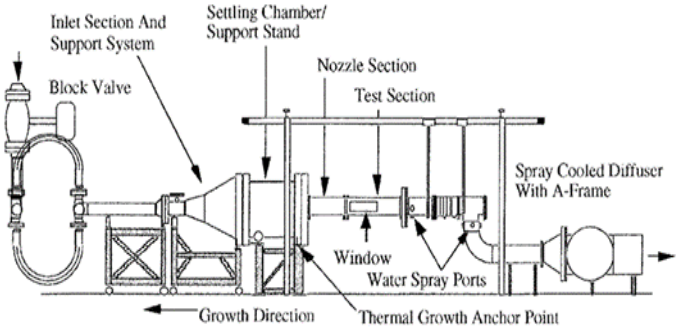

Fig.2. Experimental setup

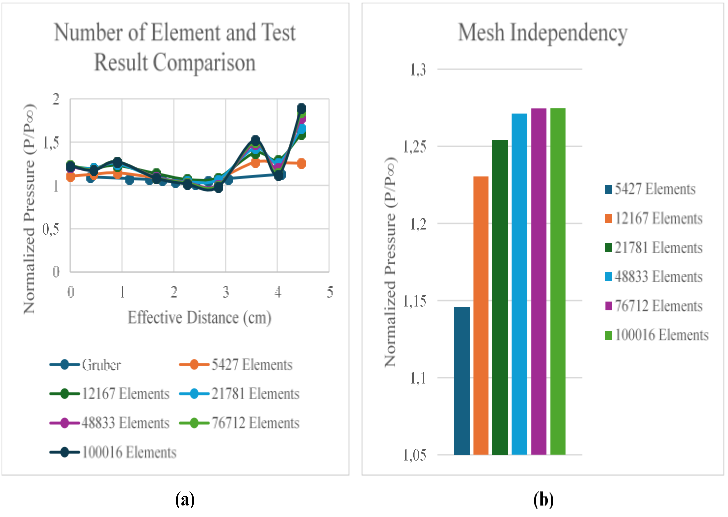

Fig.3. (a) Experimental and CFD results [18]. (b) Element number comparison

3.1. Cavity Geometry Validation

A detailed geometric analysis was performed to determine the optimal cavity configuration for effective flame stabilization in supersonic flow. Two critical geometric parameters were examined: the offset ratio (Du/D) and the rear wall ramp angle (θ). The offset ratio, defined as the ratio of the front to rear wall lengths, was evaluated at values of 1, 2, and 3. The comparison of normalized cavity pressure for these cases is shown in Figure 4, indicating that Du/D = 1 yields the highest pressure buildup within the cavity region. This pressure enhancement corresponds to stronger recirculation and increased fuel residence time—factors known to support stable combustion. Contour plots of pressure, velocity, and temperature for each offset ratio are presented in Figure 5 (a-c), where Du/D = 1 clearly demonstrates superior vortex formation and thermal buildup in the cavity, further supporting its selection.

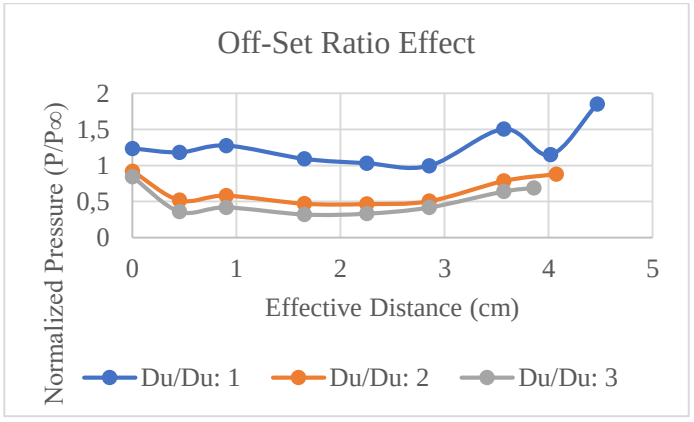

Fig.4 Comparison of O.R.

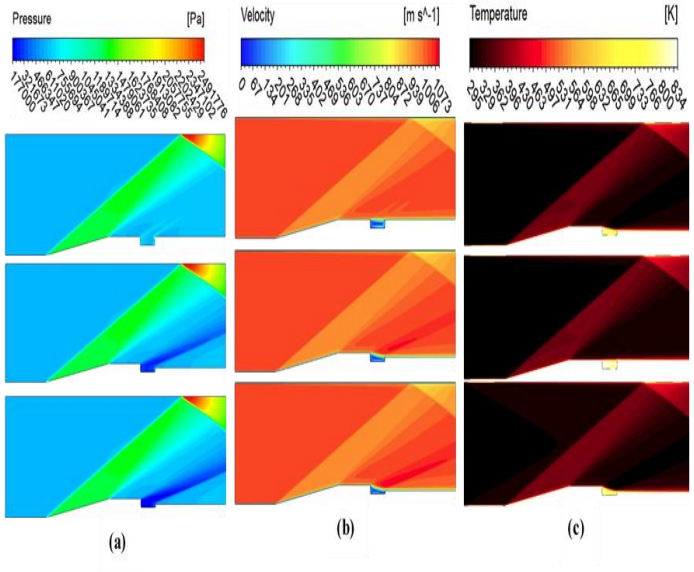

Fig.5. (a) Pressure contours of different O.R. (b) Velocity contours of different O.R. (c) Temp. contours of different O.R.

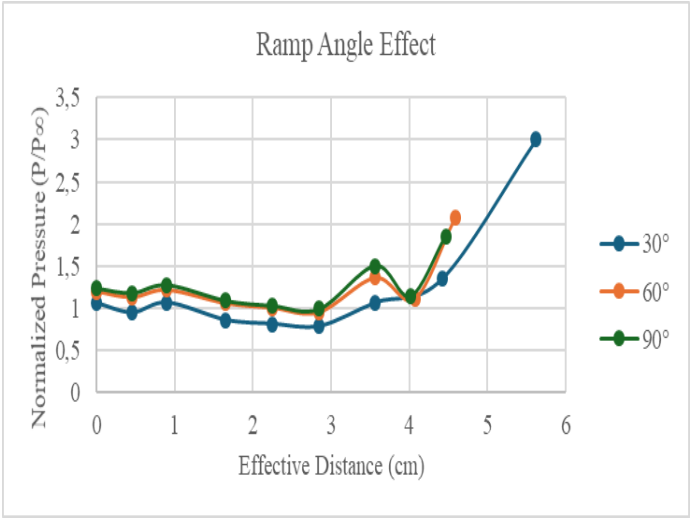

Fig.6. Comparison of ramp angles

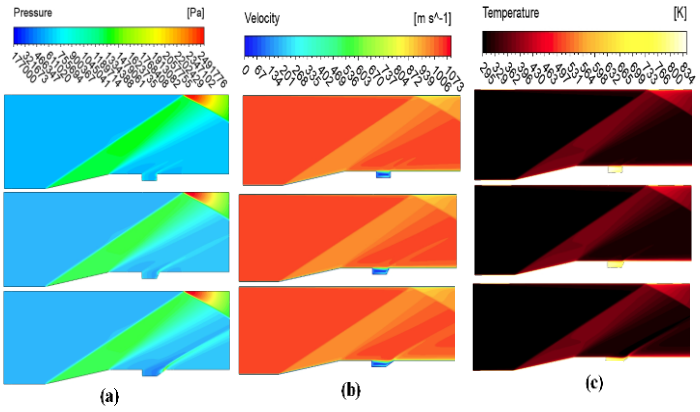

Fig.7. (a) Pressure contours of different ramp angles (b) Velocity contours of different ramp angles (c) Temp. contours of different ramp angles.

After identifying Du/D = 1 as optimal, the influence of the rear wall ramp angle was investigated by comparing 90°, 60°, and 30° configurations. As shown in Figure 6, which compares normalized pressure across these ramp angles, the differences were marginal. Although the 30° case displayed slight flow non-uniformities near the trailing edge, as seen in the contour plots of Figures 3.2.6 to 3.2.8, the overall pressure, velocity, and temperature distributions remained largely consistent across all angles. These findings confirm that while the offset ratio significantly impacts cavity performance, the ramp angle plays a secondary role. Therefore, the rectangular cavity with Du/D = 1 and rear wall angles of 90° and 60° was selected for subsequent combustion analysis and parametric studies.

4. VALIDATION PARAMETRIC STUDIES

To evaluate the influence of injector placement and pressure on combustion performance, a parametric investigation was carried out using the validated rectangular and trapezoidal cavity geometries. The configuration of both cavity types, along with the location of top, middle, and bottom injectors, is depicted in Figure 8. Each case was analyzed at three injection pressures (1 atm, 2 atm, and 3 atm), and the results are interpreted through pressure, velocity, temperature, and hydrogen concentration contours. These four variables collectively describe the flameholding potential and fuel–air mixing efficiency in supersonic conditions.

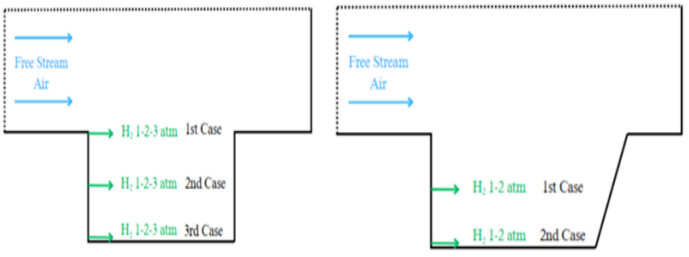

Fig.8. Rectangular and trapezoidal cavity configuration

At 1 atm injection pressure, bottom injection yielded the most effective flame anchoring conditions. The pressure distribution was more uniform and elevated within the cavity compared to middle and top injection, which suffered from underdeveloped recirculation zones and low cavity pressure. Velocity contours confirmed strong vortex formation only in the bottom configuration, which promoted enhanced fuel residence and mixing. Correspondingly, temperature fields showed high thermal intensity concentrated near the cavity step, indicating robust combustion. Hydrogen distribution maps also revealed that bottom injections enable dense and uniform fuel mixing across the cavity. These trends, which are visualized in the four sub-contours of Figure 9, support the conclusion that bottom injection at 1 atm provides the most favorable aerodynamic and thermochemical characteristics for flame stabilization.

Increasing the injection pressure to 2 atm enhanced overall performance, particularly for the middle injection configuration. Compared to 1 atm, both pressure and temperature contours showed improved flameholding conditions, with middle injection producing the highest internal cavity temperature. Velocity fields reflected fully developed recirculation with a more symmetric flow pattern in the middle injection case, while bottom injection retained strong mixing behavior with slightly reduced thermal uniformity. Hydrogen concentration fields, especially in the cavity core, were denser and more uniformly distributed in the

middle injection case [19]. These combined effects, captured in Figure 10, suggest that 2 atm injection from the middle position achieves optimal balance between mixing efficiency and combustion stability.

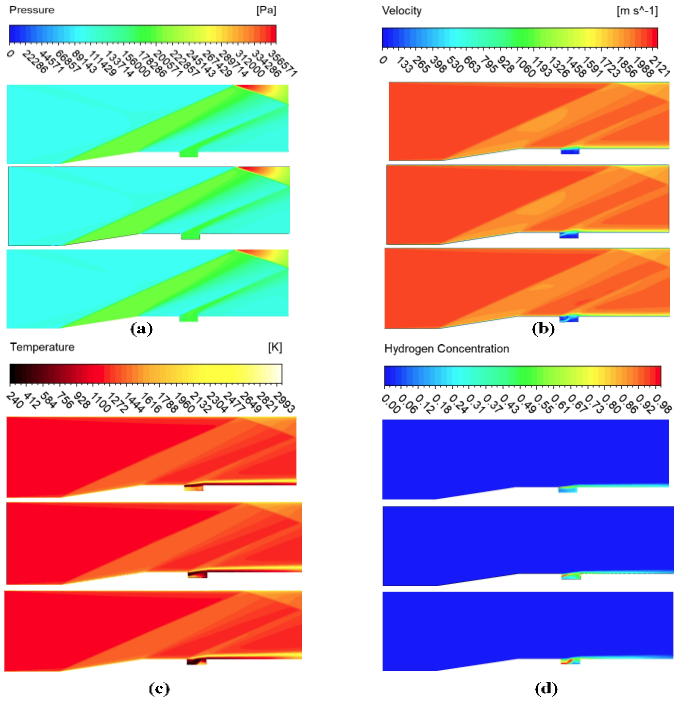

Fig.9. The three injection location at 1 atm (a) Pressure contours (b) Velocity contours (c) Temp. contours. (d) Hydrogen concentration.

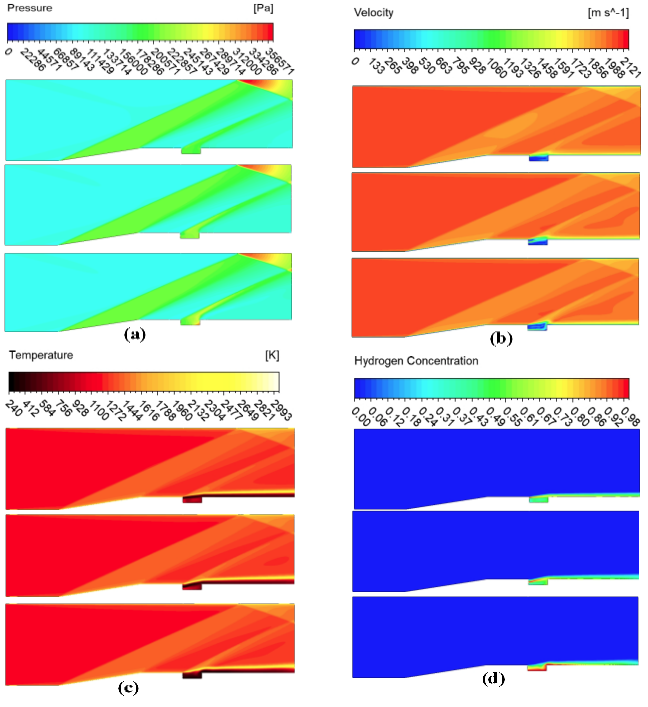

Fig.10. The three injection location at 2 atm (a) Pressure contours (b) Velocity contours (c) Temp. contours. (d) Hydrogen concentration.

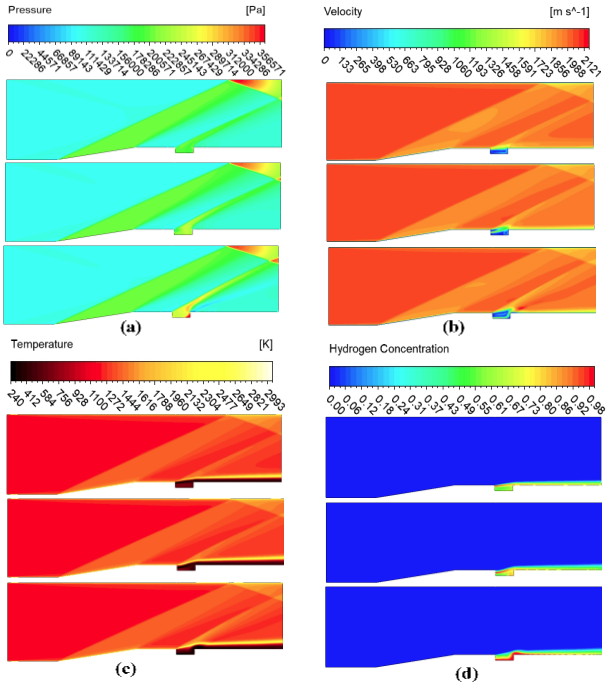

Fig.11. The three injection location at 3 atm (a) Pressure contours (b) Velocity contours (c) Temp. contours. (d) Hydrogen concentration.

At 3 atm injection pressure, performance began to deteriorate. Although pressure levels within the cavity increased further, the gradients became non-uniform and less stable, particularly in the bottom and middle injector configurations. The resulting pressure asymmetry introduced adverse flow structures, weakening the flameholding zone. Velocity contours demonstrated distorted recirculation, and temperature fields failed to show significant improvement over the 2 atm case. In fact, the temperature rise plateaued, and the hydrogen distribution became less compact and uneven. These findings, which are illustrated in Figure 11, indicate that excessive injection pressure can negatively affect flow stability and combustion uniformity, with diminishing returns above 2 atm.

Analysis of the 60° trapezoidal cavity geometry at 1 atm injection pressure demonstrated that both middle and bottom injector configurations produced viable flow recirculation. However, middle injection resulted in more homogeneous pressure distribution and temperature fields, while bottom injection concentrated combustion near the cavity base with higher thermal peaks. Velocity fields for both cases revealed functional vortex structures, although those from the bottom injection extended deeper into the cavity. Hydrogen concentration was denser in the lower cavity region for bottom injection, whereas middle injection promoted a more distributed mixture across the cavity center. These results, synthesized in Figure 12, suggest that middle injection may provide improved balance between stability and mixture uniformity in trapezoidal cavities operating at lower pressures.

At 2 atm, the trapezoidal geometry showed further improvements in combustion behavior. Both middle and bottom injection cases achieved strong and stable recirculation zones, as observed from velocity and hydrogen distribution contours. Pressure gradients remained smooth, and temperature fields revealed high thermal intensity distributed more evenly across the cavity length. Importantly, middle injection allowed the fuel to remain centered within the cavity, supporting enhanced residence time and mixing quality. These behaviors are documented in Figure 13, which highlights the enhanced flameholding and combustion efficiency attainable with moderate-pressure injection in optimized cavity geometries. Compared to the rectangular cavity, the trapezoidal form provided slightly lower peak temperatures but demonstrated more stable fuel retention and reduced thermal stress near solid boundaries.

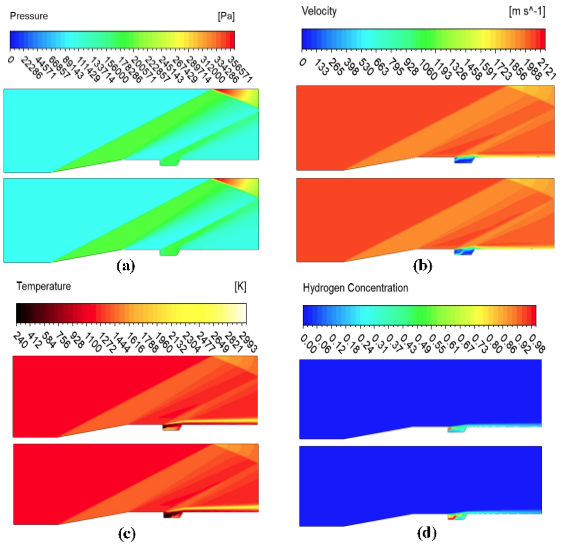

Fig.12. The Mid and Bottom Injection location of 60° backwall at 1 atm (a) Pressure contours (b) Velocity contours (c) Temp. contours. (d) Hydrogen concentration.

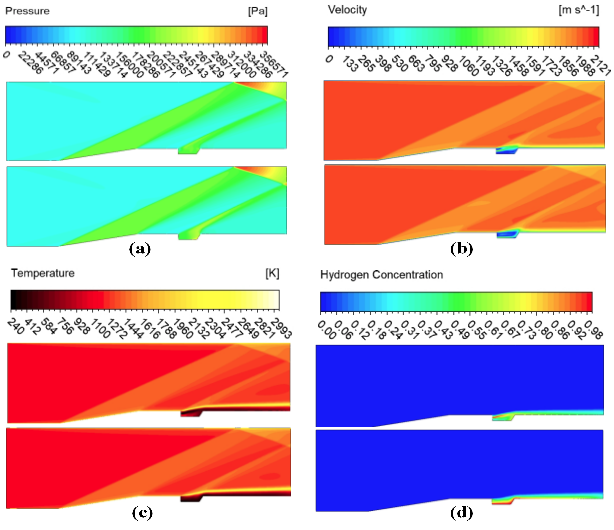

Fig.13. The Mid and Bottom Injection location of 60° backwall at 2 atm (a) Pressure contours (b) Velocity contours (c) Temp. contours. (d) Hydrogen concentration.

5. CONCLUSION

This study presented a comprehensive CFD-based investigation into the effects of cavity geometry and fuel injection configuration on flame stabilization in supersonic scramjet combustors. Two cavity types rectangular and trapezoidal were evaluated through parametric variations in offset ratio, ramp angle, injection location, and injection pressure. The simulation results validated against experimental data and subjected to mesh independence checks revealed significant dependencies between cavity design, injector setup, and combustion behavior.

Among the tested geometries, the rectangular cavity with an offset ratio of Du/D = 1 demonstrated the most effective vortex formation and pressure retention, supporting its selection for detailed analysis. While variations in ramp angle had a negligible impact on combustion-relevant flow fields, injection location and pressure were found to be critical. The middle injection at 2 atm provided the most balanced combination of pressure stability, thermal development, and fuel retention. This configuration consistently yielded strong recirculation, high combustion efficiency, and uniform hydrogen mixing. In contrast, top injection failed to promote adequate fuel-air interaction, and increasing the injection pressure to 3 atm did not produce significant performance benefits in some cases, it introduced flow instability.

Comparative analyses also indicated that the 60° trapezoidal cavity geometry, while slightly less efficient thermally, offered improved mixture distribution and lower thermal gradients along cavity walls. This may be advantageous in reducing thermal stress and material fatigue in practical applications.

Overall, the findings highlight the critical role of cavity design and injector strategy in determining scramjet combustor performance. The identified configuration rectangular cavity, centerline injection at 2 atm provides a promising design baseline for future experimental validation and hardware development. Future studies may extend these findings by incorporating angled or pulsed injection strategies, as well as exploring multi-element cavity interactions under transient flow conditions.

REFERENCES

[1] X. Li, Q. Lei, X. Zhao, W. Fan, S. Chen, L. Chen, Y. Tian and Q. Zhou, "Combustion Characteristics of a Supersonic Combustor with a Large Cavity Length to Depth Ratio," *Aerospace*, vol. 9, no. 4, p. 214, 2022.

[2] S. Huang, Q. Chen, Y. Cheng, J. Xian and Z. Tai, "Supersonic Combustion Modeling and Simulation on General Platforms," *Aerospace*, vol. 9, no. 7, p. 366, 2022.

[3] G. B. Goodwin, R. F. Johnson, D. A. Kessler, A. D. Kercher and H. K. Chelliah, "Effect of Inflow Turbulence on Premixed Combustion in a Cavity Flameholder," arXiv preprint, arXiv:2001.05893, 2020. [Online]. Available: https://arxiv.org/abs/2001.05893

[4] M. Lin, J. Fang, X. Deng, X. Gu and Z. X. Chen, "Direct numerical simulation of inflow boundary-layer turbulence effects on cavity flame stabilisation in a model scramjet combustor," Aerosp. Sci. Technol., vol. 165, p. 110463, 2025.

[5] E. B. Jeong, S. O'Byrne, I. S. Jeung and A. F. P. Houwing, "The Effect of Fuel Injection Location on Supersonic Hydrogen Combustion in a Cavity Based Model Scramjet Combustor," *Energies*, vol. 13, no. 1, p. 193, 2020.

[6] Y. Zhang, Y. Chen and Y. Sun, "Numerical and experimental examination of strut plus wall injection in a scramjet combustor," *Advances in Mechanical Engineering*, Springer, 2025.

[7] Y. Sun, F. Li, J. Zhu *et al.*, "Effects of Additional Cavity Floor Injection on Ignition and Combustion in a Mach 2 Supersonic Flow," *Energies*, vol. 13, no. 18, p. 4801, 2020.

[8] Z. Liu *et al.*, "Ignition and flame stabilization in an ethylene-fueled cavity stabilized scramjet engine," *Proc. EUCASS Conf.*, 2022.

[9] N. Relangi, A. Ingenito and S. Jeyakumar, "Implications of Injection Locations in an Axisymmetric Cavity-Based Scramjet Combustor," *Energies*, vol. 14, p. 2626, 2021.

[10] F. Li, M. Sun, Z. Cai, Y. Chen, Y. Sun, F. Li and J. Zhu, "Effects of additional cavity floor injection on the ignition and combustion processes in a Mach 2 supersonic flow," Energies, vol. 13, no. 18, p. 4801, 2020

[11] Y. Zhang, Y. Chen and Y. Sun, "Characteristics of Flame Stabilization Enhancement in a Strut Based Supersonic Combustor," *Advances in Mechanical Engineering*, Springer, 2025.

[12] X. Li *et al.*, "Supersonic Combustion Mode Analysis of a Cavity Based Scramjet," *Aerospace*, MDPI, 2022.

[13] Z. Meng, C. Shen, K. Jia and H. He, "Numerical study on flame stabilization by shock-induced in a supersonic combustor with parallel-cavity: Symmetric configuration," Acta Astronaut., vol. 232, pp. 721–733, 2025

[14] B. Lukovic, P. Orkwis, M. Turner and B. Sekar, "Effect of cavity L/D variations on neural network-based deterministic unsteadiness source terms," in Proc. 40th AIAA Aerospace Sciences Meeting & Exhibit, Reno, NV, USA, 2002, p. 857, AIAA Paper 2002-0857.

[15] G. Choubey, M. Solanki, T. Bhatt, G. Kshitij, D. Yuvarajan and W. Huang, "Numerical investigation on a typical scramjet combustor using cavity floor H2 fuel injection strategy," *Acta Astronautica*, vol. 202, pp. 373–385, Jan. 2023.

[16] M. R. Gruber, R. A. Baurle, T. Mathur and K. Y. Hsu, "Fundamental studies of cavity-based flameholder concepts for supersonic combustors," *Journal of Propulsion and Power*, vol. 17, no. 1, pp. 146–153, 2001.

[17] M. Yüzücü, "Numerical Investigation of the Effect of Flameholder Geometry on Air-Fuel Mixing in Scramjet Engines," M.S. thesis, 2024.

[18] Z. Cai, M. Sun, Z. Wang and X. S. Bai, "Effect of cavity geometry on fuel transport and mixing processes in a scramjet combustor," *Aerospace Science and Technology*, vol. 80, pp. 309–314, Sep. 2018.

[19] T. Roos, A. Pudsey, M. Bricalli and H. Ogawa, "Cavity enhanced jet interactions in a scramjet combustor," *Acta Astronautica*, vol. 157, pp. 162–179, Apr. 2019.